Non-Contrast MR Angiography: Flow-Sensitive Dephasing (FSD)-Prepared 3D Balanced SSFP

Zhaoyang Fan[1]; Rola Saouaf[2]; Xin Liu[3]; Xiaoming Bi[4]; Debiao Li[1]

[1]Biomedical Imaging Research Institute, Cedars-Sinai Medical Center, Los Angeles, CA, USA
[2]Imaging Department, Cedars-Sinai Medical Center, Los Angeles, CA, USA
[3]Lauterbur Research Center for Biomedical Imaging, Shenzhen Institutes of Advanced Technology of Chinese Academy of Sciences, Shenzhen, China
[4]Siemens Healthcare, MR R&D, Los Angeles, CA, USA

Introduction

Contrast-enhanced MR angiography (CE-MRA) has become a non-invasive modality of choice for detecting arterial disease across various vascular regions. However, patients with renal insufficiency who receive gadolinium-based agents are at risk for developing a debilitating and potentially fatal disease known as nephrogenic systemic fibrosis (NSF) [1, 2]. As a result, a substantial population in need for angiogram will not be able to benefit from this radiation-free, non-invasive diagnostic tool. Furthermore, with CE-MRA, short contrast first-pass window in arteries often limits the imaging coverage and/or spatial resolution, and venous contamination may be present at distal run-off vessels. All limitations above, along with added cost of contrast agent, have triggered a renaissance of interest in non-contrast MRA (NC-MRA).

Time-of-flight and phase-contrast are two original NC-MRA techniques, but not widely accepted for imaging peripheral arteries, primarily due to the limited spatial coverage (or time inefficiency) as well as well-known flow artifacts associated with complex flow [3]. Recently, a group of NC-MRA techniques, such as fast spin-echo based fresh blood imaging (FBI) methods (also known as NATIVE SPACE on Siemens systems) [4], quiescent interval single-shot (QISS) [5] or Ghost [6], have been developed as an alternative to CE-MRA for peripheral MRA. Among them, balanced steady-state free precession (SSFP) using flow-sensitive dephasing (FSD) magnetization preparation* is a non-contrast approach that provides several unique features including high arterial blood SNR and blood-tissue CNR, isotropic sub-millimeter spatial resolution, and flexible FSD module to suppress flow in different directions and with different speeds [7]. The clinical feasibilities of this method have been demonstrated in lower legs [8, 9], feet [10], and hands [11, 12]. Given its potentially broad applications and rising research and clinical interests, this work provides an overview of underlying principles and technical considerations followed by clinical research results.

*Work in progress. The product is still under development and not commercially available yet. Its future availability cannot be ensured.

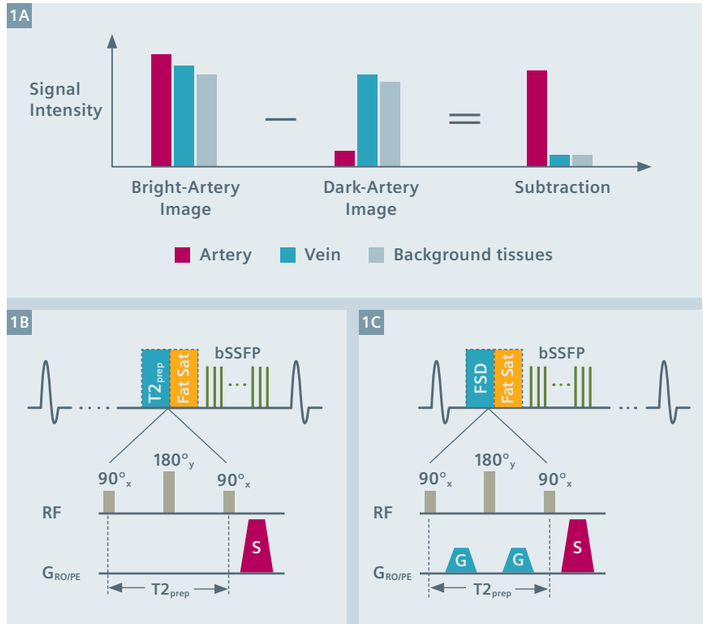

1 **(1A)** Schematic of the FSD-prepared balanced SSFP technique. In the bright-artery acquisition, both arterial blood, venous blood, and other tissues are of high signal intensity. In the dark-artery measurement, arterial blood signals are mostly suppressed by FSD-preparation because of substantially fast flow. Thus, arterial blood signals remain and the signals of venous blood and background tissues are essentially cancelled out upon image subtraction.
(1B) The sequence diagram of the bright-artery acquisition (T2-prepared balanced SSFP).
(1C) The sequence diagram of the dark-artery acquisition (FSD-prepared balanced SSFP). G = FSD gradients, S = spoiler gradients.

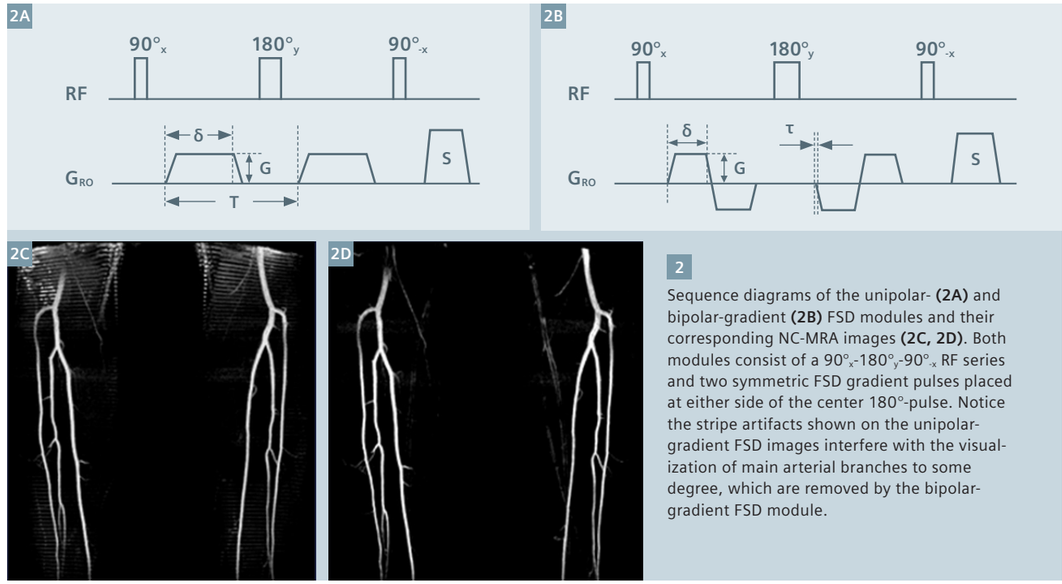

2 Sequence diagrams of the unipolar- **(2A)** and bipolar-gradient **(2B)** FSD modules and their corresponding NC-MRA images **(2C, 2D)**. Both modules consist of a $90°_x$-$180°_y$-$90°_x$ RF series and two symmetric FSD gradient pulses placed at either side of the center 180°-pulse. Notice the stripe artifacts shown on the unipolar-gradient FSD images interfere with the visualization of main arterial branches to some degree, which are removed by the bipolar-gradient FSD module.

Principles

The FSD-prepared balanced SSFP method exploits the arterial pulsatility and introvoxel spin dephasing effect to selectively depict arterial flow. The similar idea dates back to 1980s by Wedeen et al. [13] and Meuli et al. [14]. In brief, two consecutive ECG-triggered acquisitions are acquired in one scan (Fig. 1A). The bright-artery measurement is acquired with a zero-gradient-strength FSD preparation (i.e. T2 preparation) during diastole when arterial flow is substantially slow and thus retains high signal intensity on balanced SSFP images (Fig. 1B). The dark-artery measurement is collected during systole exploiting the marked velocity difference between arterial and venous flows. An optimal FSD preparation is employed to intravoxelly dephase the arterial blood spins while having little effect on venous blood and static tissues (Fig. 1C). Magnitude subtraction of the two measurements allows the visualization of arteries with dramatically suppressed background and venous signals.

Technical considerations

FSD gradient waveform

The FSD pulse sequence is a $90°_x$-$180°_y$-$90°_{-x}$ driven equilibrium Fourier transform diffusion preparation module, and identical field gradients are applied symmetrically around the 180° radio-frequency (RF) pulse [15]. Analysis based on the Bloch equation reveals that conventional unipolar-gradient pulses (Fig. 2A) in the FSD module can introduce a spatial signal modulation in static tissues, as shown below, if the center 180° RF pulse frequency response is spatially inhomogeneous.

$$M_z = (-\cos\Theta \sin^2\Phi + \cos^2\Phi) \times M_0 \quad [1]$$

$$\Phi(r) = \gamma \times r \times A \quad [2]$$

where M_z is the longitudinal magnetization right after FSD-preparation, M_0 is the equilibrium magnetization, Θ is the actual flip angle of the 180°-pulse, Φ is the phase the static spins accumulate during the FSD gradient before the 180°-pulse, which is dependent of the gradient's net area A, r is the spatial variable along the gradient direction, and γ is the gyromagnetic ratio. The period, λ,of the spatial signal modulation is defined as:

$$\lambda = \frac{\pi}{\gamma \times A} \quad [3]$$

A simple solution to circumventing the issue is to have Φ,or A, equal to zero. A bipolar-gradient scheme (Fig. 2B) becomes a natural choice to achieve this goal. Example images using the two gradient waveforms are shown in figures 2C and D.

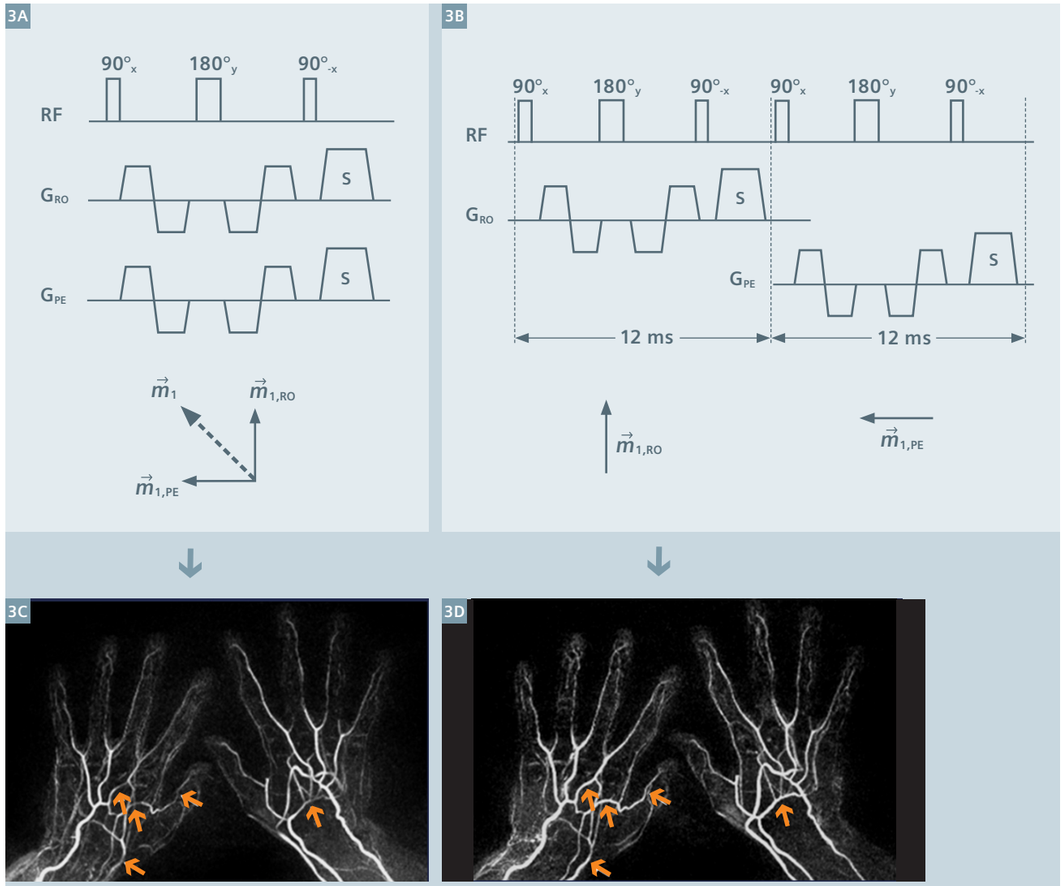

3 Sequence diagrams and example images using the single-module FSD preparative scheme versus two-module FSD preparative scheme. Notice that signal defects are observed at several arterial segments (arrows, generally located at the 90° with respect to the vector sum of the readout and phase-encoding directions) on single module-based NC-MRA, which are dramatically improved on two module-based NC-MRA.

Choice of the FSD strength

Flow sensitization imparted by the FSD preparation is essential for the NC-MRA technique, and its strength can be measured by the first-order gradient moment denoted as m_1 [7]. An unnecessarily large m_1 value may entail signal contamination from venous blood and, potentially, other static background tissues due to the associated diffusion effect, whereas incomplete delineation of arterial segments may result from an inadequate m_1 value. Consequently, a suboptimal m_1 tends to cause poor image quality, overestimation of stenosis, or false diagnosis in FSD MRA.

The optimal m_1, however, is subject and artery specific since dephasing of flowing spins is not only dependent on the m_1 of the FSD preparation but also on the local flow velocity profile [7, 16]. To obtain a satisfied MR angiogram, an empirical m_1 value derived from a pilot study can be advantageous. A more effective and reliable way is to first conduct an m_1-scout scan that can rapidly (within 1 min) assess a range of first-order gradient moment values at their effectiveness in blood signal suppression, and an individually-tailored m_1 is then selected for FSD NC-MRA scans [17].

Choice of the direction of FSD sensitivity

Intravoxel spin dephasing requires that flowing spins have the flow components along the direction of applied FSD gradients. Compared to other NC-MRA techniques, a unique feature with FSD preparation is the flexibility in direction in which the signal of flow is exclusively suppressed. FSD gradients have been applied in all three logic axes simultaneously in order to impart flow sensitization to all dimensions for vessel wall imaging in previous work [18-20]. Such gradient pulse configuration essentially renders the flow-sensitization unidirectional,

as derived from the vector sum of all FSD gradients. In case of FSD-prepared MRA, the signal of a coherent flow that is perpendicular to this direction will not be effectively nulled. Thus, the conventional FSD module may result in a suboptimal vessel segment depiction on MR angiograms.

To achieve signal suppression of multi-directional blood flow, we proposed a multi-directional FSD preparative scheme. Specifically, two (or three for three-dimensional flow) conventional FSD preparative modules are applied in series, with balanced FSD gradients applied along the RO direction in the first module and along the PE direction in the second one (Fig. 3) [21]. The spoiler gradients applied at the end of the preceding FSD module ensure that dephased flow spin components will not be rephased in the subsequent one. Thus, flow components along individual directions can be suppressed independently by their corresponding modules. Figure 3 shows an example whereby certain signal loss on MIP MRA was observed at several arterial segments when using the conventional single FSD module. Such signal defects mimicking vessel narrowing can be markedly ameliorated by the two-module FSD preparation.

Clinical applications

Clinical feasibility of using the FSD-based NC-MRA technique has been demonstrated in multiple arterial stations, including lower legs [8, 9], feet [10], and hands [11, 12]. In all of past studies, CE-MRA was used as a comparison reference, reflecting the fact that invasive x-ray angiography is not commonly performed in clinical diagnostic imaging routines.

At lower legs, Lim et al. [8] showed that FSD-based NC-MRA is more robust to arterial flow variations than fast spin-echo based techniques and "can be performed first line at 1.5T where exogenous contrast agents are undesirable or contraindicated". In this work, FSD-based MRA demonstrated satifactory image quality, excellent negative predictive value (91.7%), and good sensitivity (80.3%), specificity (81.7%), and diagnostic accuracy (81.3%) for hemodanymically significant (≥ 50%) stenosis. Another study by Liu et al. [9] showed that the number of diagnostic segments is not significanlty between FSD-based NC-MRA and CE-MRA, although the image quality of NC-MRA is slightly lower with signifcance reached. Similarly, high diagnostic accuracy was obtained using the NC-MRA technique. An exmaple case from [9] is shown in figure 4.

Pedal arteries present a few challenges to NC-MRA techniques, including small caliber size, relatively slow flow, and more tortuous anatomy. FSD-based NC-MRA has recently been successfully applied to diabetic patients who have foot vascular complications [10]. This work demonstrated that the NC-MRA technique can yield a significantly higher number of diagnostic arterial segments

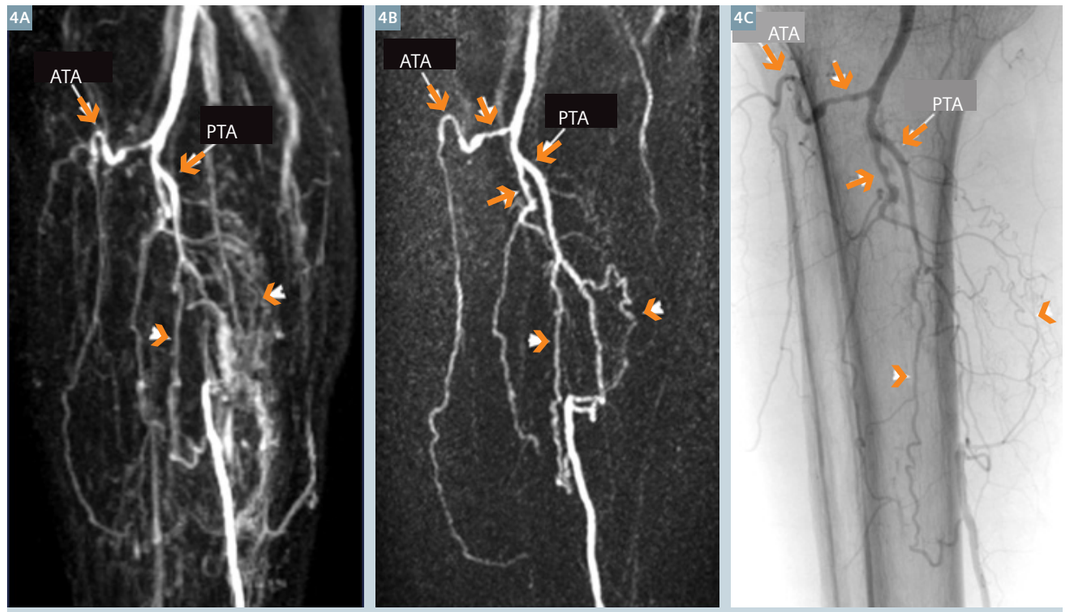

4 CE-MRA **(4A)** and NC-MRA **(4B)** MIP images and x-ray angiography image **(4C)** of the right upper calf in a 65-year-old woman with diabetes. NC-MRA clearly depicts luminal narrowing at the proximal anterior tibia artery (ATA) and peroneal artery consistent with X-ray angiography (arrows). Also, NC-MRA clearly depicts collaterals (arrowheads) with less venous contamination compared to CE-MRA in the location of a complete occlusion of proximal posterior tibia artery (PTA).

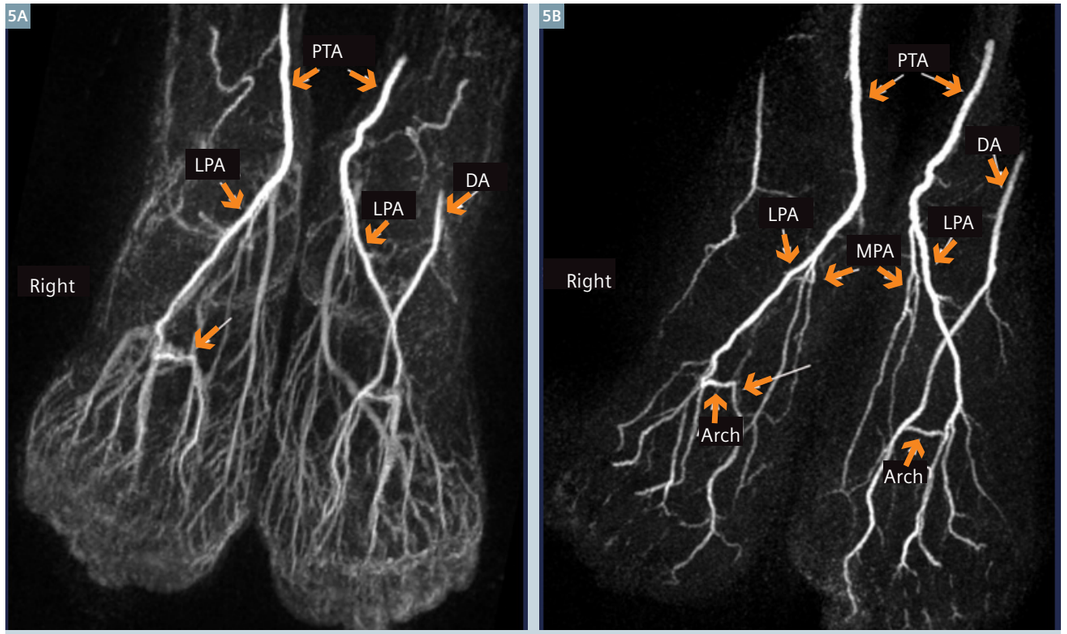

5 CE-MRA **(5A)** and NC-MRA **(5B)** MIP images of bilateral feet in a 64-year-old female with diabetes. Compared to CE-MRA images, NC-MRA shows excellent delineation of foot arteries without venous contamination. ATA = anterior tibia artery, PTA = posterior tibia artery, DA = dorsal pedal artery, LPA = lateral plantar artery, MPA = medial plantar artery, Arch = pedal arch

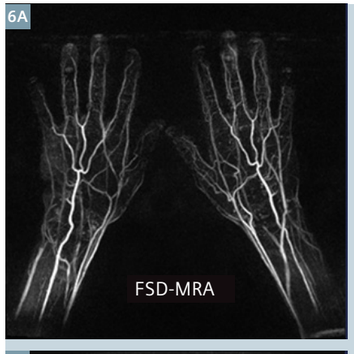

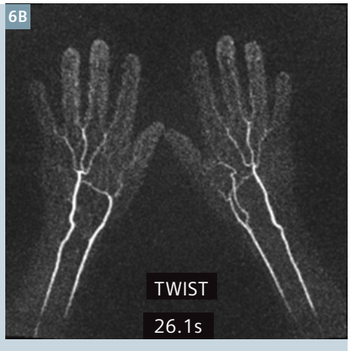

6
A 33-year-old female with SLE for 13 years and hand symptoms for 10 years. FSD demonstrates excellent visualization of the palmar vessels and excellent to good visualization of the digital vessels. There is mild venous contamination which does not affect the diagnostic quality of the images. TWIST images have good separation of arterial and venous phases but relatively poor opacification of digital vessels. CE-MRA has very good resolution but significant venous contamination limiting visualization of digital vessels.

compared to CE-MRA (93% vs. 65%). The average image quality score of NC-MRA is also significantly higher. An exmaple case from [10] is shown in figure 5.

Additionally, FSD-based NC-MRA has also found a unique application in patients with autoimmune disorders characterized by vasculopathies in hands. Lesions are primarily involved in proper digital arteries, and the diagnostic performance of CE-MRA can be compromised in imaging this station whereby small vessel caliber and short arteriovenous transit times present competing demands of high spatial resolution and short imaging time [22]. The pilot study of Reynaud phenomenon by Sheehan et al. [11] showed that FSD-based NC-MRA yield a lower degree of stenosis as compared with both high-resolution static CE-MRA and time-resolved CE-MRA, suggesting that "FSD findings may be more accurate determinants of vessel diameter". When utilizing the multi-directional FSD scheme, our recent investigation of systemic lupus erythematosus disease demonstrated that FSD-based NC-MRA is superior to CE-MRA in visulizing arterial segments in all hand vascular regions, and particularly the 3rd terminal digital arteries are much better depicted [12]. A clincal case from this work is shown in figure 6.

Conclusion

FSD-based balanced SSFP is a promising NC-MRA approach to the diagnosis of peripheral arterial disease in various vascular regions. This method eliminates the intravenous injection of contrast medium and prevents adverse contrast reaction and complications while reducing the medicla expense. Most importantly, the use of this approach in clinical practice will greatly benefit patients with impaired kidney function. Preliminary patient studies have demonstrated very promising clinical value. However, this technique still awaits clinical validations with large-size patient population to establish itself as a routine non-contrast MRA diagnostic tool.

Acknowledgements

The authors are grateful to the colleagues from Siemens Healthcare, especially Renate Jerecic, Sven Zuehlsdorff, and Gehard Laub.

References

1 Thomsen HS. Nephrogenic systemic fibrosis: A serious late adverse reaction to gadodiamide. *Eur Radiol* 2006; 16:2619-21.
2 Marckmann P, Skov L, Rossen K, et al. Nephrogenic systemic fibrosis: suspected causative role of gadodiamide used for contrast-enhanced magnetic resonance imaging. *J Am Soc Nephrol* 2006;17:2359-62.
3 Miyazaki M, Lee VS. Nonenhanced MR angiography. Radiology 2008; 248:20-43.
4 Miyazaki M, Sugiura S, Tateishi F, et al. Non-contrast-enhanced MR angiography using 3D ECG-synchronized half-Fourier fast spin echo. *J Magn Reson Imaging* 2000;12:776-83.
5 Edelman RR, Sheehan JJ, Dunkle E, et al Quiescent-interval single-shot unenhanced magnetic resonance angiography of peripheral vascular disease: Technical considerations and clinical feasibility .Magn Reson Med 2010; 63:951-8.
6 Koktzoglou I, Edelman RR. Ghost Magnetic Resonance Angiography. Magnetic Resonance in Medicine, 2009, 61:1515–1519.
7 Fan Z, Sheehan J, Bi X, et al. 3D noncontrast MR angiography of the distal lower extremities using flow-sensitive dephasing (FSD)-prepared balanced SSFP. Magn Reson Med 2009; 62:1523-32.
8 Lim RP, Fan Z, Chatterji M, et al. Comparison of nonenhanced MR angiographic subtraction techniques for infragenual arteries at 1.5 T: A preliminary study. Radiology 2013; 267:293-304.
9 Zhang N, Fan Z, Feng F, et al. Clinical evaluation of peripheral non-contrast enhanced MR angiography (NCE-MRA) using steady-state free precession (SSFP) and flow sensitive dephasing (FSD) in diabetes. In Proceedings of the 20th Annual Meeting of ISMRM, Melbourne, Victoria, Australia, 2012; p. 730.
10 Fan Z, Liu X, Zhang N, et al. Non-contrast enhanced MR angiography (NCE-MRA) of the foot using flow sensitive dephasing (FSD) prepared steady-state free precession (SSFP) in patients with diabetes. In Proceedings of the 21st Annual Meeting of ISMRM, Salt Lake City, Utah, USA, 2013; p.5799.
11 Sheehan JJ, Fan Z, Davarpanah AH, et al. Nonenhanced MR angiography of the hand with flow-sensitive dephasing-prepared balanced SSFP sequence: initial experience with systemic sclerosis. Radiology 2011; 259:248-56.
12 Saouaf R, Fan Z, Ishimori ML, et al. Comparison of noncontrast FSD MRA to time resolved (TWIST) and high resolution contrast enhanced MRA of the hands in patients with systemic lupus erythematosus (SLE) and clinical vasculopathy. In Proceedings of the 21st Annual Meeting of ISMRM, Salt Lake City, Utah, USA, 2013; p.3963.
13 Wedeen VJ, Meuli RA, Edelman RR, et al. Projective imaging of pulsatile flow with magnetic resonance. Science 1985; 230:946 –948.
14 Meuli RA, Wedeen VJ, Geller SC, et al. MR gated subtraction angiography: evaluation of lower extremities. Radiology 1986; 159:411– 418.
15 Becker ED, Farrar TC. Driven equilibrium Fourier transform spectroscopy. A new method for nuclear magnetic resonance signal enhancement. J Am Chem Soc 1969; 91:7784-7785.
16 Haacke EM, Brown RW, Thompson MR, Venkatesan R. Magnetic resonance imaging physical principles and sequence design. New York: Wiley-Liss; 1999, pp. 673.
17 Fan Z, Zhou X, Bi X, et al. Determination of the optimal first-order gradient moment for flow-sensitive dephasing magnetization-prepared 3D noncontrast MR angiography. Magn Reson Med 2011; 65:964-72.
18 Sirol M, Itskovich VV, Mani V, et al. Lipid-rich atherosclerotic plaques detected by gadofluorine-enhanced in vivo magnetic resonance imaging. Circulation 2004; 109:2890-2896.
19 Koktzoglou I, Li D. Diffusion-prepared segmented steady-state free precession: Application to 3D black-blood cardiovascular magnetic resonance of the thoracic aorta and carotid artery walls. J Cardiovasc Magn Reson 2007; 9:33-42.
20 Wang J, Yarnykh VL, Hatsukami T, et al. Improved suppression of plaque-mimicking artifacts in black-blood carotid atherosclerosis imaging using a multislice motion-sensitized driven-equilibrium (MSDE) turbo spin-echo (TSE) sequence. Magn Reson Med 2007; 58:973-981.
21 Fan Z, Hodnett P, Davarpanah A, et al. Noncontrast magnetic resonance angiography of the hand: Improved arterial conspicuity by multidirectional flow-sensitive dephasing (FSD) magnetization preparation in 3D balanced steady-state free precession imaging. Investigative Radiology 2011; 46:515-523.
22 Connell DA, Koulouris G, Thorn DA, Potter HG. Contrast-enhanced MR angiography of the hand. Radiographics 2002; 22:583-599.

Contact

Debiao Li, Ph.D.
Cedars-Sinai Medical Center
116 N. Robertson Blvd,
Suite 800
Los Angeles, CA 90048
USA
Phone: +1 310-423-7743
debiao.li@cshs.org